Desalination and Water Treatment
www.deswater.com
doi: 10.5004/dwt.2021.26619

212 (2021) 434–443
February

Effective magnetic separation of phosphate from natural water by a novel magnetic composite

Yuanfu Ma, Chen Wang*, Qing Feng

School of Environmental Science and Engineering, Qilu University of Technology (Shandong Academy of Sciences), Jinan 250353, China, emails: shanqing123@126.com (C. Wang), 18021779037@163.com (Y. Ma), qingfeng@qlu.edu.cn (Q. Feng)

Received 8 May 2020; Accepted 27 September 2020

ABSTRACT

In this study, we aimed to magnetically separate phosphate from natural water and change its source-to-sink conversion to prevent eutrophication. To this end, a promising material in terms of phosphate removal efficiency and magnetic separability was developed. Nine types of magnetic composite P-removal agents were prepared by changing the types of metal salts (i.e., Zn^{2+}, Cu^{2+}, Mg^{2+}, Al^{3+}, Fe^{3+}, Zr^{4+}, Y^{3+}, Ce^{3+}, and La^{3+}), and the optimal agent was determined to be La^{3+}/poly (acrylamide-co-acryloyloxyethyl thimethylammonium chloride)/Fe_3O_4 [La^{3+}/CPAM/Fe_3O_4] based on phosphate removal efficiency. The optimal synthesis conditions, including reaction time (4 h), reaction temperature (65°C), and the content of metal salts (12.96 mmol), were determined. The synthesized material was characterized by transmission electron microscopy, X-ray photoelectron spectroscopy, Fourier-transform infrared spectroscopy, X-ray diffraction, and vibrating-sample magnetometry. The results showed that the material featured a core–shell structure and exhibited good magnetic response. The experimental results showed that the removal process was rapid and completed within 20 min. Moreover, the material could greatly reduce P concentration, with phosphate removal efficiency reaching 90.07%. This material could effectively separate phosphate under the action of an external magnetic field and change the source-to-sink conversion of P, thereby preventing the risk of eutrophication.

Keywords: Eutrophication control; Phosphate elimination; Magnetic separation; Source-to-sink conversion; Natural water

1. Introduction

Phosphorus (P) is an essential element of all life forms [1]. Excess P is generally considered to be an important factor for eutrophication in natural water [2]. Eutrophication has been a global environmental problem in natural water, such as in lakes, marshes, and reservoirs [3]. In recent years, great progress has been made in limiting P inputs from the point and non-point contaminant sources [4,5]. External P is released into natural water from sediment, which is deposited at the bottom of the water and serves as a sink of internal P [6]. Therefore, the ability of sediment in natural water to reduce constant P input is limited. Under a variety of complex environmental conditions such as high or low pH environments and redox conditions, P in the sediment will be re-released to the overlying water [7]. Eventually, the sink of internal P becomes the internal source of eutrophication in natural water. The conversion of P in sediment and overlying water occurs annually in natural water. Furthermore, the P concentration in natural water is not reduced mainly because the source-to-sink conversion of P remains unchanged.

Traditional techniques such as sediment dredging, hypolimnetic aeration, and chemical precipitation have been applied to prevent the release of P from sediment in natural water [8,9]. However, sediment dredging is based

* Corresponding author.

on various preconditioning methods involving an additional expensive infrastructure [10]. The main drawback of hypolimnetic aeration is its high energy cost. Chemical precipitation is another method for reducing the P concentration in natural water, and it has attracted increasing attention because of its high efficiency and stability [11]. However, it requires the consumption of large quantities of chemicals and inevitably produces large quantities of precipitates [12]. The P in these precipitates is re-released into the overlying aqueous phase due to the aging of the chemicals and the complex environmental conditions [13]. To reduce the risk of eutrophication in natural water, effectively preventing the source-to-sink conversion of P in the sediment and the overlying water is critical. Some scholars have controlled the P concentration in overlying water by *in-situ* capping technology. However, P is not separated from the natural waters and may thus be re-released [14]. Changing the source-to-sink conversion of P in natural water is difficult using traditional methods. Therefore, new methods for effectively separating P from natural water must be explored.

In recent years, magnetic composite materials have been gaining increasing attention due to their unique magnetic properties [15]. Magnetic iron oxide has magnetic properties and low toxicity, and it is easier to separate from natural water than other non-magnetic materials. In some studies [16,17], magnetic composite materials were used to remove dyes, and these materials had high removal efficiencies and recyclability. In addition, some scholars used magnetic composites to remove toxic heavy metals in aqueous solutions [18,19]. There have been a few studies on the separation of P from natural water using magnetic composite materials. Nevertheless, those studies normally used complex methods and expensive materials [20]. Thus, herein, P-removal chemicals were magnetized by hybridization with biocompatible magnetic materials through molecular design, after which they were combined with soluble orthophosphorus to form magnetic P-containing insoluble materials (henceforth referred to as insolubles). Under the action of an external magnetic field, the magnetic P-containing insolubles were attracted to the magnet and could be magnetically separated from natural water. This method is highly efficient and stable because it is based on chemical precipitation. Furthermore, it avoids the large amounts of sludge produced by traditional chemical precipitation methods. Using this method, the source-to-sink conversion of P in natural water can be hindered, and the risk of eutrophication can be avoided.

In this study, a magnetic composite agent for P-removal was first prepared by aqueous solution polymerization. The optimal synthesis conditions for preparing the magnetic composite agent were determined by an orthogonal experimental design, and the best agent was determined. The magnetic composite agent exhibited suitable selective removal of P, and the influences of the pH value, coexisting ions, and initial P concentration, were evaluated. Moreover, the interaction mechanism of the magnetic composite agent and phosphates was investigated by Fourier-transform infrared (FT-IR) spectroscopy and X-ray photoelectron spectroscopy (XPS). X-ray diffraction (XRD) analysis was carried out using a D8 ADVANCE with Cu Kα radiation (30 kV, 15 mA). The particle size and saturation magnetization of the agent were characterized by transmission electron microscopy (TEM) and vibrating-sample magnetometry (VSM), respectively.

2. Materials and methods

2.1. Materials

All the chemicals used for the preparation of the magnetic composite P-removal agent were commercially available and were used without further purification. Acrylamide (AM), ammonium persulfate ($(NH_4)_2S_2O_8$), and zinc sulfate heptahydrate ($ZnSO_4 \cdot 7H_2O$) were supplied by Tianjin Damao Reagent Co., Ltd., (Tianjin, China). Ferrous sulfate septihydrate, sodium bisulfite ($NaHSO_3$), and gelatin were purchased from Tianjin Bodi Chemical Co., Ltd., (Tianjin, China). Moreover, *N*,*N*-dimethylaminoethyl acrylate methyl chloride quaternary (DAC, 80%) was supplied by Wanduoxin Chemical Co., Ltd., (Jinan, China). Citric acid, magnesium chloride hexahydrate ($MgCl_2 \cdot 6H_2O$), aluminum chloride hexahydrate ($AlCl_3 \cdot 6H_2O$), and ferric chloride hexahydrate ($FeCl_3 \cdot 6H_2O$) were obtained from Sinopharm Chemical Reagent Co., Ltd., Shanghai, China. Lanthanum chloride heptahydrate ($LaCl_3 \cdot 7H_2O$) and cupric chloride ($CuCl_2$) were purchased from Shanghai Macklin Biochemical Co., Ltd., China. Cerium chloride heptahydrate ($CeCl_3 \cdot 7H_2O$), yttrium chloride heptahydrate ($YCl_3 \cdot 7H_2O$), and zirconium sulfate tetrahydrate ($Zr(SO_4)_2 \cdot 4H_2O$) were supplied by Shanghai Aladdin Reagent Co., Ltd., China. Monopotassium phosphate (KH_2PO_4) was obtained from Tianjin Kemiou Chemical Reagent Co., Ltd., China.

2.2. Synthesis of magnetic composite P-removal agent

Magnetite (Fe_3O_4) nanoparticles and poly (AM-co-DAC)–grafted (CPAM) gelatin were successfully prepared in the laboratory [21,22]. The synthesis conditions of the magnetic composite P-removal agent were optimized by orthogonal experiments. Different types of magnetic composite P-removal agents were prepared by changing the types of metal salts (i.e., Zn^{2+}, Cu^{2+}, Mg^{2+}, Al^{3+}, Fe^{3+}, Zr^{4+}, Y^{3+}, Ce^{3+}, and La^{3+}) under the best condition, and the best metal ions were determined based on phosphate removal efficiency. The metal ions were supplied by the metal salts, which could combine with phosphate to form P-containing substances. Therefore, the influence of the quantities of metal salts on phosphate removal efficiency was investigated. Moreover, the reaction time and reaction temperature could affect the completion and stability of the agent. Therefore, the agent specimens with various reaction conditions were obtained by altering the reaction time (factor *A*), reaction temperature (factor *B*), and amount of metal salt (factor *C*). It was assumed that no correlation existed between any two factors. An orthogonal matrix L9 (3^3) was used, and the levels are presented in Table 1.

First, Fe_3O_4 (1.5 g) and the reagents for preparing the poly(AM-co-DAC)-g-gelatin were placed in a three-necked flask and reacted at 80°C for 130 min. The reaction temperature of the system was then changed according to the designed conditions. Next, predetermined amounts of metal salt were added and reacted for a suitable time. The final product was extracted with ethanol and dried at 40°C until the weight was constant.

Table 1
Levels and factors in orthogonal experimental design

Factors	Levels			
	Factors	1	2	3
Reaction time, (h)	*A*	2	4	6
Reaction temperature, (°C)	*B*	50	65	80
Amount of metal salt, (mmol)	*C*	6.48	12.96	19.44

2.3. Characterization of materials

The size and structure of the magnetic composite P-removal agent were inspected using a TEM (JEOL, JEM-1400, Tokyo, Japan). The surface elemental composition of the magnetic composite P-removal agent was analyzed using an X-ray photoelectron spectrometer (Bruker, D8-ADVANCE, Beijing, China) with an Al kα radiation source (1,486.6 eV). All the binding energies of the XPS spectra were recorded by calibrating the graphitic carbon C1 s peak at 284.6 eV. The functional groups of the hybrid polymers were determined using an FT-IR spectrometer (Shimadzu, IRAffinity-1s, Japan). The spectrum for each sample, collected as the average of over 128 scans, was taken from 400 to 4,000 cm^{-1} at a resolution of 4 cm^{-1}. The XRD analysis was carried out using a D8 ADVANCE with a Cu Kα radiation source (30 kV, 15 mA). The magnetic properties of the samples were measured using a vibrating sample magnetometer (Lake Shore 7404, USA) at room temperature.

2.4. Batch experiments

Phosphate removal experiments were conducted to investigate the phosphate removal performances of the magnetic composite P-removal agent. The phosphate concentration was determined using the ammonium molybdate method with a UV-vis spectrometer (PERSEE, TU-1901, Beijing, China). The initial pH of the phosphate stock solution was adjusted using 0.1 M HCl or 0.1 M NaOH. The samples in the phosphate solution with an initial concentration of 50 mg/L were stirred at 150 rpm for 30 min. After the phosphate removal experiments, samples were filtered through 0.45 μm mixed-cellulose membrane filters, and the filtrate was collected for further analysis. To investigate the influence of the dosage of the magnetic composite agent on phosphate removal efficiency, batch experiments were carried out by adding various concentrations of the agent at pH 7.0 ± 0.1. The influence of pH on the phosphate removal efficiency of the agent was studied, and a certain dosage of the agent was added to solutions with different initial pH levels, ranging from 3.0 to 12.0 for the batch experiments. To investigate the influence of competitive anions on phosphate removal efficiency, batch experiments were conducted by adding certain amounts of competing anions (NO_3^-, HCO_3^-, SO_4^{2-}, and Cl^-) to the phosphate solutions at pH 7.0 ± 0.1 in separate beakers. The molar ratios of phosphate to competitive anions were 1:1, 1:20, and 1:100. The influences of parameters such as the amount of P-removal agent, reaction time, and initial phosphate concentration were investigated. Phosphate removal efficiency (R, %) was calculated using the following equation:

$$R(\%) = \left(\frac{C_0 - C_f}{C_0}\right) \times 100 \tag{1}$$

where C_0 and C_f are the initial and final concentrations of the phosphate (mg/L).

3. Results and discussion

3.1. Optimization strategy of orthogonal experiment

The data from the orthogonal experiments were analyzed to better clarify the relationship between the experimental conditions and results. For example, La^{3+} was used to prepare the magnetic composite P-removal agent (La^{3+}/CPAM/Fe_3O_4) and investigate phosphate removal efficiency under different experimental conditions. Nine selected experiments were used in an L9 (3^3) orthogonal table, and the results are shown in Table 2. These experiments were designed to optimize the synthesis conditions of the magnetic composite P-removal agent and increase phosphate removal efficiency.

The maximum and minimum phosphate removal efficiencies of La^{3+}/CPAM/Fe_3O_4 were observed to be 88.86% and 67.19%, respectively. The parameter K_i (i = 1, 2, and 3) denotes the average value of phosphate removal efficiency in the equal levels of each factor, and R is the interval between the maximum and minimum K_i values. Moreover, the value of R could be used to evaluate the extent to which various factors influenced phosphate removal efficiency. A larger R indicates that the factor had a more significant effect on the phosphate removal efficiency [23]. The R values of factors A, B, and C were 0.567, 4.294, and 15.471, respectively. Therefore, among these three factors, the amount of metal salt had the greatest impact on phosphate removal efficiency, followed by the reaction temperature, and the reaction time had the weakest impact. The analysis of variance (ANOVA) results are presented in Table 3. In addition, phosphate removal efficiency was investigated by changing the La^{3+} proportion in the La^{3+}/CPAM/Fe_3O_4 for the phosphorus solution treatment. Phosphate removal efficiency was significantly increased by increasing the amount of added lanthanum salt. This directly indicated that phosphate removal efficiency had a positive correlation with the quantity of La^{3+} in the La^{3+}/CPAM/Fe_3O_4. For a given statistical significance level, the standard F-value was determined using an F-table [24]. If the F-variance ratio was higher than the standard F-value, the corresponding factors would contribute significantly to the experimental results. As for the inspection level, $\alpha = 0.05$, $F_{(2,2)} = 19$, and $F_{(C)} = 59.615$. Thus, $F_{(C)} > F\alpha$. Furthermore, according to the ANOVA results, factor C played the most important role in phosphate removal efficiency, followed by factor B, which had a larger contribution than factor A. This conclusion was consistent with the range analysis.

Through the above analysis, the optimal conditions for preparing La^{3+}/CPAM/Fe_3O_4 were determined, and the agent was accordingly re-prepared for subsequent experiments. Thus, the stability and accuracy of the orthogonal experiment were verified. The results showed that the phosphate removal efficiency of La^{3+}/CPAM/Fe_3O_4 prepared under the optimal conditions was 90.07%.

Table 2
Results of orthogonal experiment

Experimental number	Factor result			
	A (h)	*B* (°C)	*C* (mmol)	Phosphate removal efficiency (%)
1	1	1	1	67.19
2	1	2	2	88.86
3	1	3	3	79.35
4	2	1	3	84.45
5	2	2	1	81.43
6	2	3	2	70.19
7	3	1	2	78.47
8	3	2	3	72.70
9	3	3	1	83.20
K_1	78.467	76.703	70.027	
K_2	78.690	80.997	85.503	
K_3	78.123	77.580	79.750	
R	0.567	4.294	15.476	
Best level	A_2	B_2	C_2	
Influence degree of factors	Amount of metal salt > reaction temperature > reaction time			

Table 3
Analysis of variance (ANOVA) of phosphate removal efficiency

Source	SS	df	*F*	*P*
A	0.486	2	0.079	0.926
B	30.875	2	5.013	0.166
C	367.171	2	59.615	0.016
Error	6.16	2		

SS: sum of squared deviations; df: degrees of freedom; F: F ratio; P: probability value test.

3.2. Determination of metal ions for preparing magnetic composite P-removal agent

Nine kinds of magnetic composite P-removal agents (M^{n+}/CPAM/Fe_3O_4) were prepared by changing the metal ions under the optimal synthesis conditions. The best metal ion was determined by comparing the phosphate removal efficiencies of these magnetic composite agents. Fig. 1 shows the phosphate removal efficiency of different types of magnetic composite P-removal agents. The dosages of the different agents were 0.75, 1.75, 2.25, 2.75, and 3.75 g/L. The phosphate removal efficiencies of these agents were compared and the best agent was selected. The results showed that the magnetic composite agents based on Fe^{3+}, Al^{3+}, Mg^{2+}, Cu^{2+}, Zn^{2+}, and Ce^{3+} had low phosphate removal efficiencies at pH = 7 ± 0.1, which limits the application of these six agents in natural water. However, under the same conditions, lanthanum-, zirconium-, and yttrium-based magnetic composite agents had relatively high phosphate removal efficiencies. Among these agents, La^{3+}/CPAM/Fe_3O_4 exhibited the highest phosphate removal efficiencies. When the dosage of La^{3+}/CPAM/Fe_3O_4 was 3.75 g/L, phosphate removal efficiency reached 90.07%.

Phosphate removal efficiency was determined by the stability and magnetic response of the magnetic insolubles formed by the magnetic composite P-removal agent and phosphates. The magnetic response of these agents was affected by the amount of Fe_3O_4. Different types of magnetic composite agents were prepared with the same amount of Fe_3O_4, and they had the same magnetic response. Therefore, the stability of the magnetic insolubles was considered to be the main factor in the study of phosphate removal efficiency. The solubilities and bond dissociation energies of the compounds formed by the combination of various metal ions and phosphates can be found in the Rankine chemistry manual. Fig. 1, the solubilities, and the bond dissociation energies of compounds formed all indicated that the lower the solubilities of the insoluble were, the higher the phosphate removal efficiencies of these agents were. The ionic radii of rare-earth ions are large, and thus, these ions could combine with more phosphate than the other metal ions, and the phosphate removal efficiencies were high [25,26]. The oxygen atoms in the phosphate radicals provided a lone electron pair that formed coordinate bonds with the unoccupied orbitals of the metal ion in the P-removal agent molecule. The stability of the coordination compound was affected by the dissociation energy of the coordination bond. The dissociation energies of the rare-earth ions combined with phosphate were greater than those of the metal ions combined with phosphate, except for zirconium ions. Therefore, the phosphate removal efficiency of the rare-earth magnetic composite P-removal agent was higher than those of the other P-removal agents. However, the famous lanthanide contraction (that causes a decline in ionic radius from 1.13 Å for La^{3+} to 1.00 Å for Lu^{3+}) resulted in a subtle change in the properties. Furthermore, due to the lanthanum ions, which were in the 4f subshell, the valence state of lanthanum was stable, and the coordination bonds formed with the ligands were firm [27]. The combination process of the magnetic composite

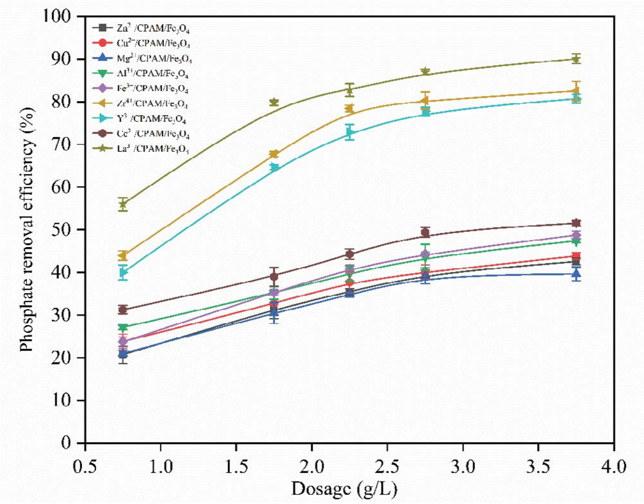

Fig. 1. Phosphate removal efficiencies of nine magnetic composite P-removal agents.

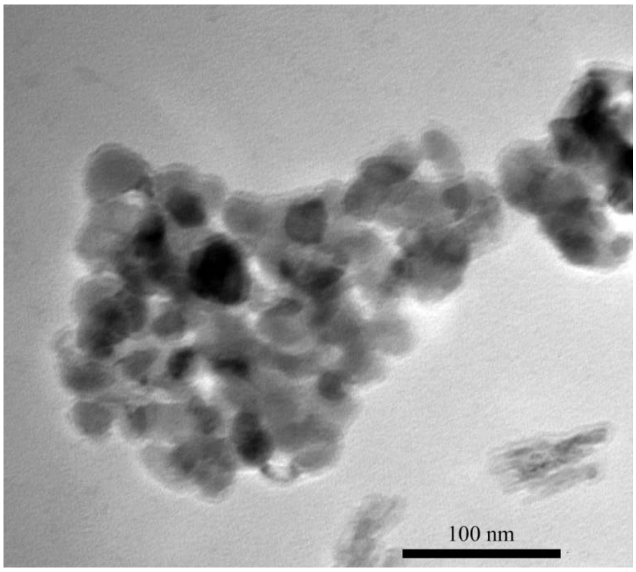

Fig. 2. TEM image of $La^{3+}/CPAM/Fe_3O_4$ nanocomposites.

P-removal agent with phosphate to form insolubles could be affected by the coexisting ions in natural water. However, due to their special electronic structures, the rare-earth magnetic composite P-removal agents had strong affinities and selectivities for phosphate [28]. Hence, the phosphate removal efficiency of $La^{3+}/CPAM/Fe_3O_4$ was higher than those of the other eight agents. Thus, $La^{3+}/CPAM/Fe_3O_4$ was selected as the best agent to remove phosphate in natural water.

3.3. Characterization of materials

3.3.1. Characterization by transmission electron spectroscopy

To determine the morphology and average size of the as-synthesized $La^{3+}/CPAM/Fe_3O_4$, the material was analyzed using TEM (Fig. 2). As shown in Fig. 2, the $La^{3+}/CPAM/Fe_3O_4$ nanoparticles were nearly spherical, with their diameters ranging from about 15 to 40 nm. During the preparation of $La^{3+}/CPAM/Fe_3O_4$, the Fe_3O_4 nanoparticles were entrapped by the macromolecular compounds, forming a core–shell-like structure. A large number of nanoparticles attracted each other and converged, due to their high surface energy and the mutual magnetic interaction of Fe_3O_4 [29].

3.3.2. Characterization by XPS

To further investigate the chemical compositions and states of $La^{3+}/CPAM/Fe_3O_4$ before and after it bonded with phosphate, XPS surface characterizations of the $La^{3+}/CPAM/Fe_3O_4$ and $La^{3+}/CPAM/Fe_3O_4$ + P were performed. Fig. 3 shows the XPS spectra of $La^{3+}/CPAM/Fe_3O_4$ and $La^{3+}/CPAM/Fe_3O_4$ + P. The pristine $La^{3+}/CPAM/Fe_3O_4$ consisted mainly of carbon, nitrogen, chlorine, lanthanum, and iron (Fig. 3a). As shown in Fig. 3b, additional photoelectron lines at a binding energy (BE) of about 132.9 eV, which were attributed to the P 2p species, appeared after phosphate removal. This phenomenon demonstrated that phosphate was successfully loaded onto the $La^{3+}/CPAM/Fe_3O_4$ [30]. The distinctly contrasting XPS spectra of the La 3d before and after phosphate removal are illustrated in Fig. 3c. The BEs of La $3d_{5/2}$ were centered at 834.7 and 838.1 eV, and the peaks of La $3d_{3/2}$ were 851.6 and 854.7 eV. After the removal process, the peaks of the La $3d_{5/2}$ and La $3d_{3/2}$ were higher (ca. 0.4–0.7 eV), indicating that electron transfer could have occurred in the valence band of La 3d, and an inner spherical complex La–O–P was formed. Similar results were also observed in a previous study of phosphate sequestration by nano-La(III) (hydr)oxide-modified wheat straw [31]. As shown in Fig. 1d, representative peaks of Fe 2p were located at 710.2 eV, which corresponded to the characteristic binding energies of Fe_3O_4. No significant change was observed in the BE of Fe 2p after phosphate removal.

3.3.3. Characterization by FT-IR spectrum analysis

The functional groups of the Fe_3O_4/CPAM, $La^{3+}/CPAM/Fe_3O_4$, and $La^{3+}/CPAM/Fe_3O_4$ + P, determined by FT-IR characterization, are compared in Fig. 4. For the $La^{3+}/CPAM/Fe_3O_4$ spectra, a large peak of the primary amine $-NH_2$ (m) was observed at 3,360 cm^{-1}, and two sharp peaks were observed for primary amide (s) and $-COO^-$ at 1,662 and 1,419 cm^{-1}, respectively. The stretching vibration peak of N^+-linked $-CH_2-N-(CH_3)_3$ was observed at 1,454 cm^{-1}. The results indicated that dimethyl groups were present in the hybrid polymers. A small peak of C–C was observed at 1,168 cm^{-1}, and a broad and low peak was found for Fe–O at 590 cm^{-1} [32]. This proved that Fe_3O_4 was present in the $La^{3+}/CPAM/Fe_3O_4$. Moreover, the $La^{3+}/CPAM/Fe_3O_4$ spectrum featured a lower peak intensity of the primary amine than the $CPAM/Fe_3O_4$ spectrum, and the range was also smaller. This was mainly due to the metal ions compounded on the $La^{3+}/CPAM/Fe_3O_4$, which hindered the absorption of infrared light. Meanwhile, a blue shift occurred at the peaks of the carboxylate group on the $La^{3+}/CPAM/Fe_3O_4$ from 1,643 and 1,392 cm^{-1} to 1,662 and 1,419 cm^{-1}, respectively, which was mainly caused by La^{3+} taking part in the reaction. Moreover, a new intense peak appeared at 1,056 cm^{-1}. This was attributed to the antisymmetric stretching vibrations of the P–O bonds

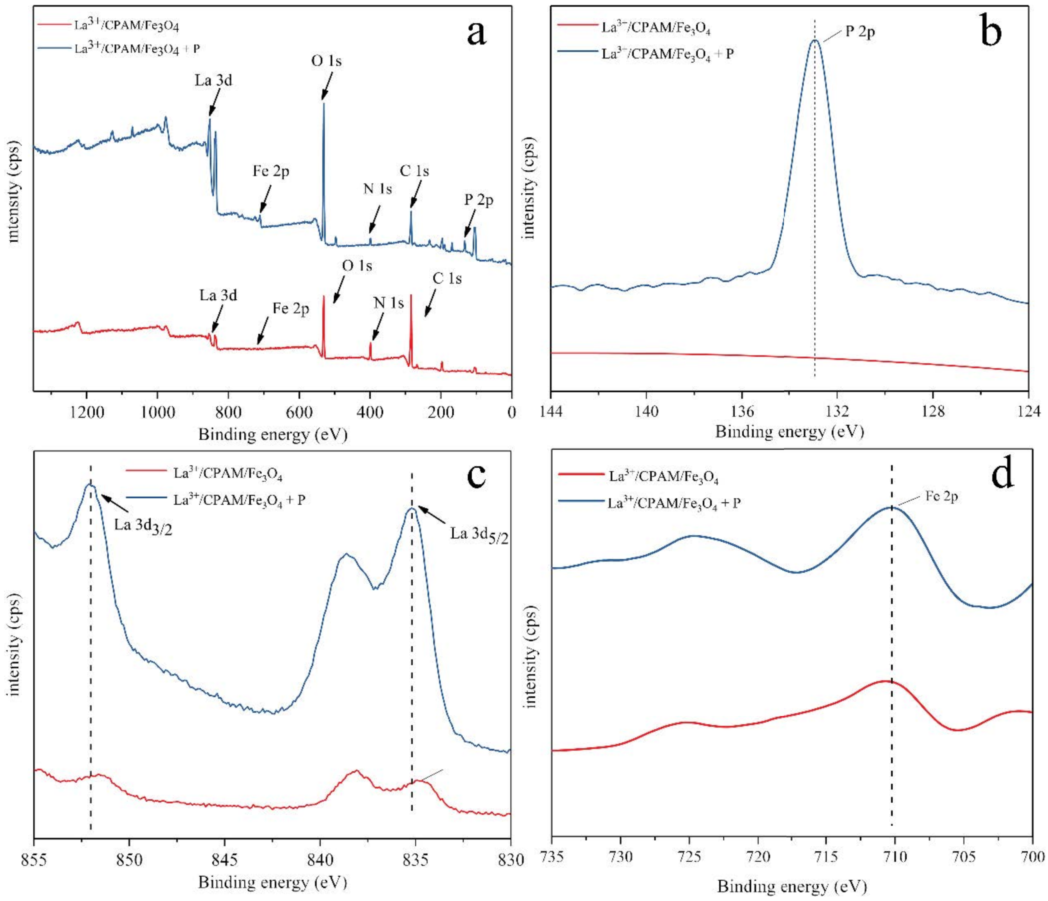

Fig. 3. (a) Wide scan, (b) P 2p, (c) La 3d, and (d)Fe 2p XPS spectra of the La^{3+}/CPAM/Fe_3O_4 and La^{3+}/CPAM/Fe_3O_4 + P at pH 7.0 ± 0.1.

[33]. After the La^{3+}/CPAM/Fe_3O_4 combined with phosphate, a new peak of the O–P–O bending modes formed at 540 cm^{-1}, which was attributed to the presence of phosphate [34].

3.3.4. Characterization by vibrating-sample magnetometry spectrum analysis

Fig. 5a shows the magnetic response of the La^{3+}/CPAM/Fe_3O_4. Under the action of the carboxylic groups, the La^{3+}/CPAM/Fe_3O_4 solution was homogeneously dispersed and attracted by an external magnet. The phenomenon indicated that the La^{3+}/CPAM/Fe_3O_4 exhibited a good dispersity and magnetic response.

The magnetic properties of the La^{3+}/CPAM/Fe_3O_4 were studied in an external magnetic field from −10 to 10 kOe. The hysteresis loops of the CPAM/Fe_3O_4 and La^{3+}/CPAM/Fe_3O_4 are shown in Fig. 5b. The results indicated that both samples exhibited superparamagnetism. The saturation magnetization values of CPAM/Fe_3O_4 and La^{3+}/CPAM/Fe_3O_4 were 1.77 and 1.66 emu/g, respectively. Increasing the La^{3+} content resulted in a smaller saturation magnetization value, which was because the non-magnetic matter attenuated the magnetization of the Fe_3O_4. Moreover, CPAM/Fe_3O_4 and La^{3+}/CPAM/Fe_3O_4 exhibited superparamagnetism, mainly because of the presence of nanoscale magnetite particles in the core [35]. This superparamagnetic La^{3+}/CPAM/Fe_3O_4

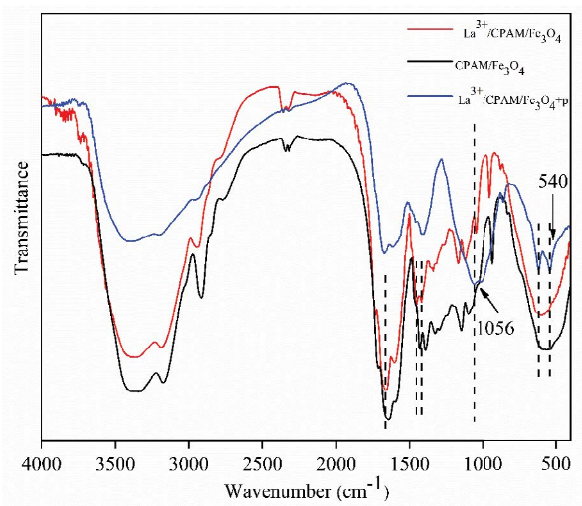

Fig. 4. FTIR spectra of the CPAM/Fe_3O_4, La^{3+}/CPAM/Fe_3O_4 nanocomposite and La^{3+}/CPAM/Fe_3O_4 + P.

with high magnetic properties could be used to achieve rapid solid–liquid separation in natural water. Fig. 5c shows the magnetic response of the final product. The La^{3+}/CPAM/Fe_3O_4 combined with phosphate to form magnetic

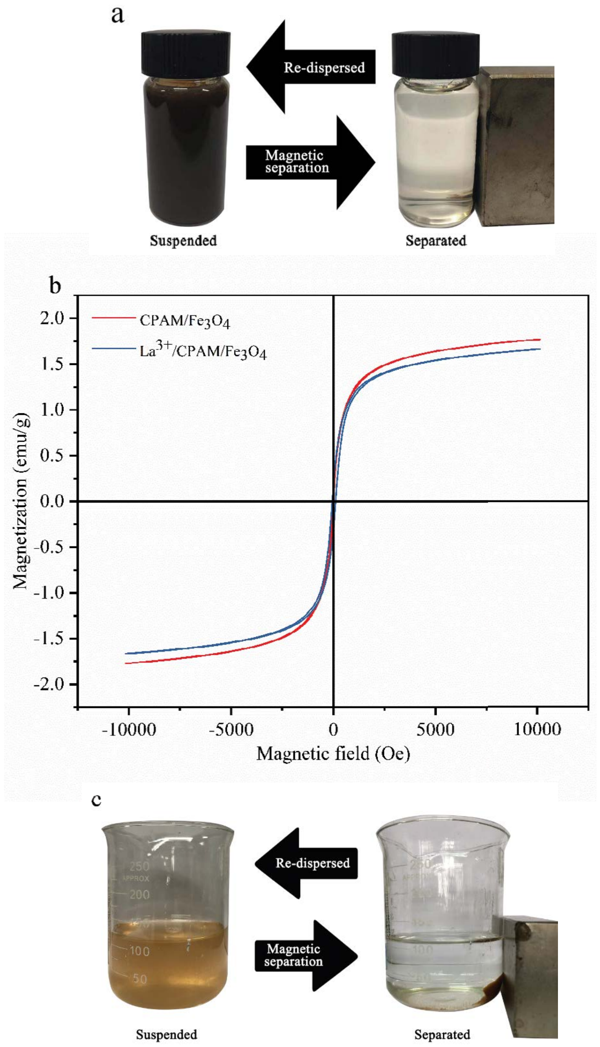

Fig. 5. (a) Magnetic separation of La^{3+}/CPAM/Fe_3O_4 under external magnetic field, (b) magnetic hysteresis loops of CPAM/Fe_3O_4 and La^{3+}/CPAM/Fe_3O_4, and (c) magnetic separation of La^{3+}/CPAM/Fe_3O_4 under an external magnetic field.

insolubles and could be attracted to a magnet placed at the side of the beaker. This phenomenon shows that solid–liquid separation could be effectively realized under the action of a magnetic field, and the P contents were removed. This advantage further promotes the practical application of La^{3+}/CPAM/Fe_3O_4 in natural water.

3.3.5. Characterization by XRD patterns

The wide-angle XRD profiles of the Fe_3O_4 and La^{3+}/CPAM/Fe_3O_4 are shown in Fig. 6. The crystal structure of Fe_3O_4 was determined based on its diffraction peaks, in which the strong peaks appeared at 2θ values of 30.1°, 35.4°, 43.1°, 57.1°, and 62.4° (JCPDS card 99-0073) [36]. After being coated with the polymer, the La^{3+}/CPAM/Fe_3O_4 particles exhibited an almost identical diffraction pattern to that of Fe_3O_4, indicating the formation of an amorphous polymer layer. This indicated that the polymer and lanthanum(III)

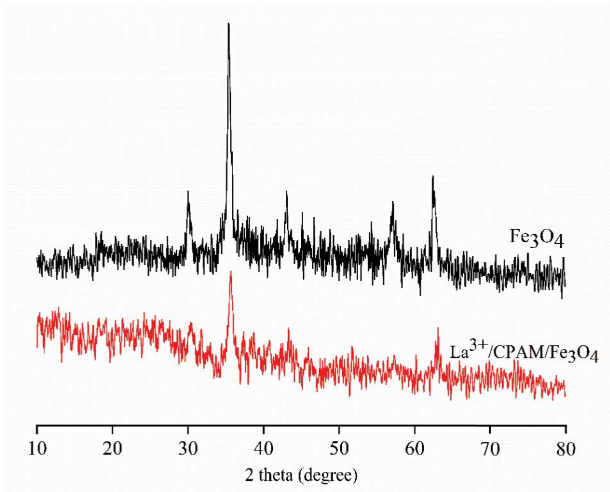

Fig. 6. XRD patterns of Fe_3O_4 and La^{3+}/CPAM/Fe_3O_4.

on the surface of Fe_3O_4 could be regarded as an amorphous phase without a crystal structure. In addition, the presence of the maghemite magnetic phase in the iron oxides with the polymer could not be excluded, because the reaction experiment was conducted in an open system. In fact, the color of the resulting magnetic composite P-removal agent could be an indication of the coexistence of magnetic maghemite. The Fe_3O_4 was black, whereas the magnetic composite P-removal agent was maroon. This result agrees with previous literature [4,37].

3.4. Effect of pH on P-removal

The effect of the initial pH on the phosphate removal by La^{3+}/CPAM/Fe_3O_4 was further investigated, and the results are illustrated in Fig. 7. When the pH was <4.0, phosphate removal efficiency was low. When the initial pH was 4–12, phosphate removal efficiency gradually increased to 100%. This phenomenon has also been observed during phosphate removal by other La-based P-removal agents [38]. The variation of the phosphate species in the aqueous solution could influence the phosphate removal efficiency of La^{3+}/CPAM/Fe_3O_4. Based on the phosphate species distribution vs. the pH, some of the H_3PO_4 was present in the aqueous solution at pH = 3. However, the H_3PO_4 state could not be effectively loaded onto the La^{3+}/CPAM/Fe_3O_4. As the pH increased from 3 to 7, the H_3PO_4 was gradually converted into monovalent $H_2PO_4^-$ species, and the $H_2PO_4^-$ could rapidly combine with La^{3+}/CPAM/Fe_3O_4. The combination could form P-containing magnetic insolubles, which improved the phosphate removal efficiency [30]. As the pH was increased to 11, the quantity of $H_2PO_4^-$ species decreased and the quantity of HPO_4^{2-} species increased. The corresponding ligand binding between HPO_4^{2-} and La^{3+}/CPAM/Fe_3O_4 was strengthened, and an intra-spherical phosphate complex was formed [28]. When the pH was increased to 12, the phosphate removal efficiency of La^{3+}/CPAM/Fe_3O_4 decreased. This result was attributed to the increased content of OH^- groups competing with HPO_4^{2-} to bind with the active sites of La^{3+}/CPAM/Fe_3O_4, thereby weakening the coordination between HPO_4^{2-} and La^{3+}/CPAM/Fe_3O_4.

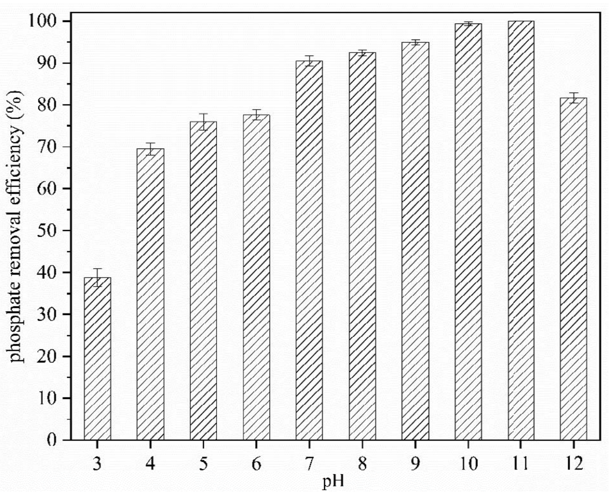

Fig. 7. Effect of solution pH on the phosphate removal efficiency by La^{3+}/CPAM/Fe_3O_4 (initial phosphate concentration: 50 mg/L; agent dosage: 3.75 g/L).

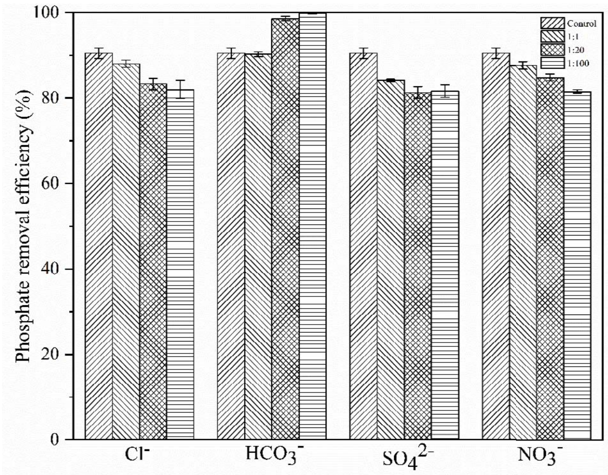

Fig. 8. Effects of various competing ions on phosphate removal efficiency by La^{3+}/CPAM/Fe_3O_4 (initial phosphate concentration: 50 mg/L; agent dosage: 3.75 g/L).

3.5. Effects of coexisting ions

Potentially competing anions such as Cl^-, HCO_3^-, SO_4^{2-}, and NO_3^-, are present in natural water, and these anions could interfere with the phosphate removal efficiency of La^{3+}/CPAM/Fe_3O_4. Therefore, to evaluate the selectivity of La^{3+}/CPAM/Fe_3O_4 for phosphate, the influences of various anions on phosphate removal efficiency were studied, and the results are presented in Fig. 8. As the molar ratios of phosphate to Cl^-, SO_4^{2-}, and NO_3^- increased to 1:100, the phosphate removal efficiency of La^{3+}/CPAM/Fe_3O_4 slightly decreased. This was because the three anions competed with the phosphate ions for the active sites of La^{3+}/CPAM/Fe_3O_4, thereby reducing phosphate removal efficiency [39]. In addition, the increase in the HCO_3^- concentration had a positive effect on the phosphate removal efficiency of La^{3+}/CPAM/Fe_3O_4. This may have been because a high $NaHCO_3$ concentration caused an increase in the electric potential at the interface, which promoted the combination of the negatively charged phosphate anions with La^{3+}/CPAM/Fe_3O_4 and was thus favorable for the magnetic separation. Moreover, sodium bicarbonate is the salt of a strong alkali weak acid, and its solution is alkaline [33,38]. Thus, the pH of the reaction system increased with the increase in the sodium bicarbonate concentration, which may have affected the existence state of phosphate and ultimately the phosphate removal efficiency of La^{3+}/CPAM/Fe_3O_4. Therefore, the strong selectivity of La^{3+}/CPAM/Fe_3O_4 to phosphate in natural water was conducive to the magnetic separation of phosphate, which further supports the application potential of La^{3+}/CPAM/Fe_3O_4 in natural water.

3.6. Influence of La^{3+}/CPAM/Fe_3O_4 dosage

To investigate the influence of the La^{3+}/CPAM/Fe_3O_4 dosage on phosphate removal efficiency, a test was conducted with an La^{3+}/CPAM/Fe_3O_4 dosage of 0.25–4.75 g/L, initial phosphate concentration of 50 mg/L, initial pH of 7, and contact time of 30 min (Fig. 9). By increasing the La^{3+}/CPAM/Fe_3O_4, the removal efficiency of phosphate increased. This was due to an increase in the number of lanthanum ions that could react with the phosphate. As shown in Fig. 9, with an increase in the dosage from 0.25 to 3.75 g/L, phosphate removal efficiency increased from 36.5% to 90.07%. As the dosage of La^{3+}/CPAM/Fe_3O_4 increased from 3.75 to 4.75 g/L, the removal efficiency of phosphate was not altered. This was mainly attributed to the precipitation reaction between La^{3+}/CPAM/Fe_3O_4 and to the phosphate reaching saturation. Since the dosage of La^{3+}/CPAM/Fe_3O_4 in the aqueous solution was constant, not all the lanthanum ion reacted with the phosphate. Furthermore, as the La^{3+}/CPAM/Fe_3O_4 dosage was increased, the removal efficiency of phosphate was reduced. When the dosage of La^{3+}/CPAM/Fe_3O_4 was in excess, the residual pH of solution changed, and the amount of phosphate decreased [40].

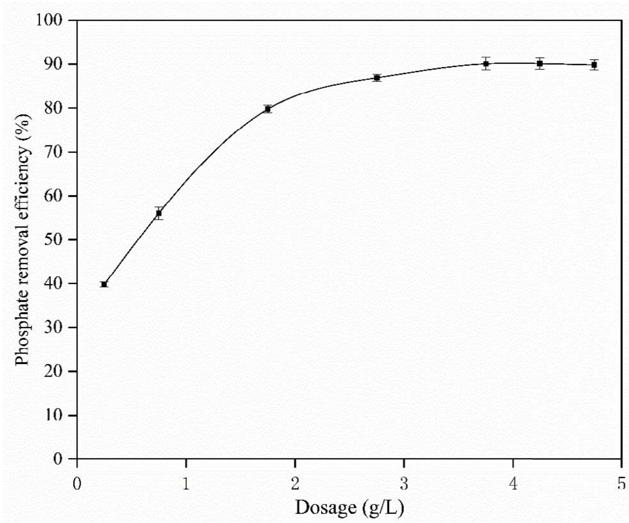

Fig. 9. Influence of La^{3+}/CPAM/Fe_3O_4 dosage on phosphate removal.

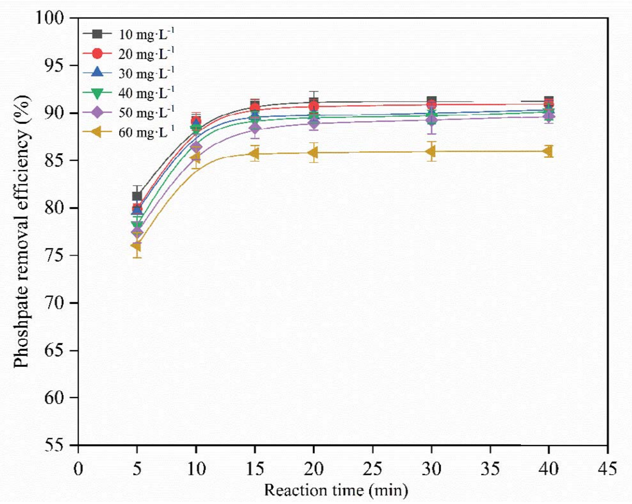

Fig. 10. Effect of reaction time and initial phosphate concentration.

3.7. Effect of reaction time and phosphate concentration

The influences of the reaction time and initial phosphate concentration on the phosphate removal efficiency of La^{3+}/CPAM/Fe_3O_4 were investigated, and the results are presented in Fig. 10. The tests were performed with a reaction time in the range of 5–40 min, an initial phosphate concentration of 10–60 mg/L, an La^{3+}/CPAM/Fe_3O_4 dose 3.75 g/L, and an initial pH of 7. Based on the results, the trends of phosphate removal efficiency were similar for all initial phosphate concentrations. By increasing the reaction time, the removal efficiency of the phosphate was performed quickly. However, after 20 min, phosphate removal efficiency was almost constant and did not change significantly. The initially high removal efficiency was attributed to the phosphate in the solution having sufficient time to react with La^{3+}/CPAM/Fe_3O_4. By increasing the reaction time, the precipitation reaction between the La^{3+}/CPAM/Fe_3O_4 and phosphate reached saturation. The optimal reaction time for the removal of phosphate was determined to be 20 min. Fig. 10 shows that the phosphate removal efficiency of La^{3+}/CPAM/Fe_3O_4 was gradually decreased by increasing the initial phosphate concentration. Due to the chemical relationship between the phosphate and P-removal agent, an increase in the phosphate concentration would cause the chemical reaction to reach saturation. After reaching saturation, excess phosphate could not be combined with the La^{3+}/CPAM/Fe_3O_4. This result agrees with previous literature [40].

4. Conclusion

In this study, a magnetic composite P-removal agent was synthesized by aqueous solution polymerization, and magnetic separation of the phosphate from the aqueous solution was achieved. The optimal magnetic composite P-removal agent was prepared with a reaction time of 4 h, a reaction temperature of 65°C, and a metal salt content of 12.96 mmol. Nine types of agents were prepared by changing the types of metal salts (i.e., Zn^{2+}, Cu^{2+}, Mg^{2+}, Al^{3+}, Fe^{3+}, Zr^{4+}, Y^{3+}, Ce^{3+}, and La^{3+}), and the optimal agent was determined to be La^{3+}/CPAM/Fe_3O_4 based on phosphate removal efficiency. The FT-IR and XPS analysis results showed that La^{3+}/CPAM/Fe_3O_4 featured a combination of La–O and Fe–O, indicating that it was successfully prepared. The TEM analysis results showed that the optimal product had a core–shell structure. In addition, the VSM results demonstrated that La^{3+}/CPAM/Fe_3O_4 exhibited a better magnetic response compared to other agents, and it could be separated from natural water under the action of an external magnetic field. Moreover, it could greatly reduce the P concentration, with phosphate removal efficiency reaching 90.07%. It also showed good selectivity to phosphate in the presence of competing anions commonly present in natural water. Overall, synthesized La^{3+}/CPAM/Fe_3O_4 is a promising material for the magnetic separation of phosphate, which could change the source-to-sink conversion of P in natural water and prevent the risk of eutrophication.

Acknowledgments

This research was supported by the Natural Science Foundation of Shandong Province, China (Grant No. ZR2014EEM044).

References

[1] M. Shams, I. Nabipour, S. Dobaradaran, B. Ramavandi, M. Qasemi, M. Afsharnia, An environmental friendly and cheap adsorbent (municipal solid waste compost ash) with high efficiency in removal of phosphorus from aqueous solution, Fresenius Environ. Bull., 22 (2013) 722–726.

[2] F. Saberzadeh Sarvestani, H. Esmaeili, B. Ramavandi, Modification of *Sargassum angustifolium* by molybdate during a facile cultivation for high-rate phosphate removal from wastewater: structural characterization and adsorptive behavior, 3Biotech, 6 (2016) 1–12.

[3] L. Fang, R. Liu, J. Li, C. Xu, L.-Z. Huang, D. Wang, Magnetite/lanthanum hydroxide for phosphate sequestration and recovery from lake and the attenuation effects of sediment particles, Water Res., 130 (2018) 243–254.

[4] L. Fang, B. Wu, I.M.C. Lo, Fabrication of silica-free superparamagnetic ZrO_2@Fe_3O_4 with enhanced phosphate recovery from sewage: performance and adsorption mechanism, Chem. Eng. J., 319 (2017) 258–267.

[5] L. Fang, Q. Shi, J. Nguyen, B. Wu, Z. Wang, I.M.C. Lo, Removal mechanisms of phosphate by lanthanum hydroxide nanorods: investigations using EXAFS, ATR-FTIR, DFT, and surface complexation modeling approaches, Environ. Sci. Technol., 51 (2017) 12377–12384.

[6] M. Søndergaard, R. Bjerring, E. Jeppesen, Persistent internal phosphorus loading during summer in shallow eutrophic lakes, Hydrobiologia, 710 (2013) 95–107.

[7] S.J. Liu, J. Li, Y.K. Yang, J. Wang, H. Ding, Influence of environmental factors on the phosphorus adsorption of lanthanum-modified bentonite in eutrophic water and sediment, Environ. Sci. Pollut. Res., 23 (2016) 2487–2494.

[8] L. Egle, H. Rechberger, J. Krampe, M. Zessner, Phosphorus recovery from municipal wastewater: an integrated comparative technological, environmental and economic assessment of P recovery technologies, Sci. Total Environ., 571 (2016) 522–542.

[9] A. Funes, J. de Vicente, L. Cruz-Pizarro, I. Álvarez-Manzaneda, I. de Vicente, Magnetic microparticles as a new tool for lake restoration: a microcosm experiment for evaluating the impact on phosphorus fluxes and sedimentary phosphorus pools, Water Res., 89 (2016) 366–374.

[10] L. Jing, X. Liu, S. Bai, C. Wu, H. Ao, J. Liu, Effects of sediment dredging on internal phosphorus: a comparative field study

focused on iron and phosphorus forms in sediments, Ecol. Eng., 82 (2015) 267–271.

[11] B. Cichy, E. Kużdżał, H. Krztoń, Phosphorus recovery from acidic wastewater by hydroxyapatite precipitation, J. Environ. Manage., 232 (2019) 421–427.

[12] L. Egle, H. Rechberger, M. Zessner, Overview and description of technologies for recovering phosphorus from municipal wastewater, Resour. Conserv. Recycl., 105 (2015) 325–346.

[13] S. Egemose, G. Wauer, A. Kleeberg, Resuspension behaviour of aluminium treated lake sediments: effects of ageing and pH, Hydrobiologia, 636 (2009) 203–217.

[14] L. Zhang, Q. Zhou, J. Liu, N. Chang, L. Wan, J. Chen, Phosphate adsorption on lanthanum hydroxide-doped activated carbon fiber, Chem. Eng. J., 185–186 (2012) 160–167.

[15] A.K. Singh, O.N. Srivastava, K. Singh, Shape and size-dependent magnetic properties of Fe_3O_4 nanoparticles synthesized using piperidine, Nanoscale Res. Lett., 12 (2017) 1–7, doi: 10.1186/s11671-017-2039-3.

[16] R. Foroutan, R. Mohammadi, J. Razeghi, B. Ramavandi, Performance of algal activated carbon/Fe_3O_4 magnetic composite for cationic dyes removal from aqueous solutions, Algal Res., 40 (2019) 101509, doi: 10.1016/j.algal.2019.101509.

[17] R. Foroutan, R. Mohammadi, B. Ramavandi, Elimination performance of methylene blue, methyl violet, and Nile blue from aqueous media using AC/$CoFe_2O_4$ as a recyclable magnetic composite, Environ. Sci. Pollut. Res., 26 (2019) 19523–19539.

[18] L. Ge, W. Wang, Z. Peng, F. Tan, X. Wang, J. Chen, X. Qiao, Facile fabrication of Fe@MgO magnetic nanocomposites for efficient removal of heavy metal ion and dye from water, Powder Technol., 326 (2018) 393–401.

[19] M. Shafiee, R. Foroutan, K. Fouladi, M. Ahmadlouydarab, B. Ramavandi, S. Sahebi, Application of oak powder/Fe_3O_4 magnetic composite in toxic metals removal from aqueous solutions, Adv. Powder Technol., 30 (2019) 544–554.

[20] H. Rashidi Nodeh, H. Sereshti, E. Zamiri Afsharian, N. Nouri, Enhanced removal of phosphate and nitrate ions from aqueous media using nanosized lanthanum hydrous doped on magnetic graphene nanocomposite, J. Environ. Manage., 197 (2017) 265–274.

[21] C. Wang, Y. Wang, Z. Ouyang, T. Shen, X. Wang, Preparation and characterization of polymer-coated Fe_3O_4 magnetic flocculant, Sep. Sci. Technol., 53 (2018) 814–822.

[22] S.K. Wang, F. Wang, Y.R. Hu, A.R. Stiles, C. Guo, C.Z. Liu, Magnetic flocculant for high efficiency harvesting of microalgal cells, ACS Appl. Mater. Interfaces, 6 (2014) 109–115.

[23] X. Wu, D.Y.C. Leung, Optimization of biodiesel production from camelina oil using orthogonal experiment, Appl. Energy, 88 (2011) 3615–3624.

[24] C. Du, Y. Hu, H. Han, W. Sun, P. Hou, R. Liu, L. Wang, Y. Yang, R. Liu, L. Sun, T. Yue, Magnetic separation of phosphate contaminants from starch wastewater using magnetic seeding, Sci. Total Environ., 695 (2019) 133723, doi: 10.1016/j.scitotenv.2019.133723.

[25] D. Copetti, K. Finsterle, L. Marziali, F. Stefani, G. Tartari, G. Douglas, K. Reitzel, B.M. Spears, I.J. Winfield, G. Crosa, P. D'Haese, S. Yasseri, M. Lürling, Eutrophication management in surface waters using lanthanum modified bentonite: a review, Water Res., 97 (2015) 162–174.

[26] P.R. Smirnov, V.N. Trostin, Structural parameters of the nearest surrounding of lanthanide ions in aqueous solutions of their salts, Russ. J. Gen. Chem., 82 (2012) 360–378.

[27] N. Antibacteria, J. He, W. Wang, F. Sun, W. Shi, D. Qi, K. Wang, R. Shi, F. Cui, Highly efficient phosphate scavenger based on well-dispersed $La(OH)_3$ nanorods in polyacrylonitrile nanofibers for nutrient-starvation antibacteria, ACS Nano, 9 (2015) 9292–9302.

[28] J. Lin, S. He, X. Wang, H. Zhang, Y. Zhan, Removal of phosphate from aqueous solution by a novel $Mg(OH)_2/ZrO_2$ composite: adsorption behavior and mechanism, Colloids Surf., A, 561 (2019) 301–314.

[29] A.M. Wahba, M. Bakr Mohamed, Structural and magnetic characterization and cation distribution of nanocrystalline $Co_xFe_{3-}xO_4$ ferrites, J. Magn. Magn. Mater., 378 (2015) 246–252.

[30] S. Dong, Y. Wang, Y. Zhao, X. Zhou, H. Zheng, $La^{3+}/La(OH)_3$ loaded magnetic cationic hydrogel composites for phosphate removal: effect of lanthanum species and mechanistic study, Water Res., 126 (2017) 433–441.

[31] H. Qiu, C. Liang, J. Yu, Q. Zhang, M. Song, F. Chen, Preferable phosphate sequestration by nano-La(III) (hydr)oxides modified wheat straw with excellent properties in regeneration, Chem. Eng. J., 315 (2017) 345–354.

[32] J. Li, C. Chen, Y. Zhao, J. Hu, D. Shao, X. Wang, Synthesis of water-dispersible Fe_3O_4@β-cyclodextrin by plasma-induced grafting technique for pollutant treatment, Chem. Eng. J., 229 (2013) 296–303.

[33] W. Gu, Q. Xie, M. Xing, D. Wu, Enhanced adsorption of phosphate onto zinc ferrite by incorporating cerium, Chem. Eng. Res. Des., 117 (2017) 706–714.

[34] L. Li, W. Jiang, H. Pan, R. Xu, Y. Tang, J. Ming, Z. Xu, R. Tang, Improved luminescence of lanthanide(III)-doped nanophosphors by linear aggregation, J. Phys. Chem. C, 111 (2007) 4111–4115.

[35] H. Chen, C. Deng, X. Zhang, Synthesis of Fe_3O_4@SiO_2@PMMA core-shell-shell magnetic microspheres for highly efficient enrichment of peptides and proteins for MALDI-ToF MS analysis, Angew. Chem. Int. Ed., 49 (2010) 607–611.

[36] Z. Wang, M. Xing, W. Fang, D. Wu, One-step synthesis of magnetite core/zirconia shell nanocomposite for high efficiency removal of phosphate from water, Appl. Surf. Sci., 366 (2016) 67–77.

[37] W.S. Peternele, V. Monge Fuentes, M.L. Fascineli, J. Rodrigues Da Silva, R.C. Silva, C.M. Lucci, R. Bentes De Azevedo, Experimental investigation of the coprecipitation method: an approach to obtain magnetite and maghemite nanoparticles with improved properties, J. Nanomater., 2014 (2014) 1–10.

[38] L. Lai, Q. Xie, L. Chi, W. Gu, D. Wu, Adsorption of phosphate from water by easily separable Fe_3O_4@SiO_2 core/shell magnetic nanoparticles functionalized with hydrous lanthanum oxide, J. Colloid Interface Sci., 465 (2016) 76–82.

[39] B. Wu, L. Fang, J.D. Fortner, X. Guan, I.M.C. Lo, Highly efficient and selective phosphate removal from wastewater by magnetically recoverable $La(OH)_3/Fe_3O_4$ nanocomposites, Water Res., 126 (2017) 179–188.

[40] W. Sun, G. Ma, Y. Sun, Y. Liu, N. Song, Y. Xu, H. Zheng, Effective treatment of high phosphorus pharmaceutical wastewater by chemical precipitation, Can. J. Chem. Eng., 95 (2017) 1585–1593.